MEASURING AND PROCESSING THE WAVEFORM OF LASER PULSES

B. Jutzi [a], U. Stilla [b]

[a] *FGAN-FOM*
Research Institute for Optronics and Pattern Recognition
Email: jutzi@fom.fgan.de

[b] *Photogrammetry and Remote Sensing*
Technische Universitaet Muenchen
Email: stilla@bv.tum.de

Abstract: The analysis of laser data to extract surface features is of great interest. Beside the range values, various information about features of the illuminated surface can be gained. In this paper, the surface features range, roughness, and reflectance are determined using different algorithms for extracting pulse properties. The accuracy of the received results is investigated by the comparison of two measurements of the same scene at different points in time to evaluate the robustness of feature extraction. The reliability and quality of the data and the used algorithms are compared and discussed.

1. Introduction

The automatic generation of 3d-models for the description of man made and natural objects, like buildings and trees, is of great interest for various applications. Beside the indirect measurement of images combined with stereoscopic analysis, active scanning laser systems offer a direct, precise, fast, and illumination independent recording of range values of 3d-objects. For topographic capturing of the ground surface with airborne systems, pulsed lasers are used typically [1,2,3].

To determine the range with a pulsed system, the time-of-flight of the laser pulses is measured, usually by employing a single characteristic property of the backscattered signal (e.g. peak detection, leading edge detection, constant fraction detection) [4]. Measurements of the backscattering characteristics from objects located at different ranges can be difficult to interpret, if they appear within a single beam footprint, leading to multiple return pulses. This kind of backscatter can appear on natural as well as on man made objects, for instance on trees with their branches and foliage or on building edges at differing heights. Depending on the application, with each emitted pulse the first or the last backscattered pulse is processed. When a threshold-based approach is used, attenuation of the signal by transmission through aerosol, fog, rain, snow, etc., reflection on a weakly backscattering cross section, or strong material absorption can produce subliminal signal values, where the detection of the object is not possible.

In contrast to the measurement of isolated range values, the recording of the complete temporal waveform and appropriate analysis offers the possibility to resolve scene related ambiguities. This analysis offers the possibility to take into account the energy and the spreading of the backscattered pulse. The examination and description of the emitted and

backscattered pulse shape under various surface conditions [5,6] are the basis for the interpretation of the recorded waveform. The prediction of the resulting waveform by simulating the illumination of a complex surface can be helpful [7]. The reliability and quality of the waveform analysis is relevant for the accuracy of change detection with pulsed laser scanner systems for monitoring purposes like rockslide, snow cover, glacier change, and plants growth.

Recent developments of laser scanner systems led to systems that allow capturing the waveform with approximately 1 GSamples/s: RIEGL LMS-Q560, LITEMAPPER 5600, OPTECH ALTM 3100, TOPEYE II. This waveform sampling rate provides a range resolution of 0.15 m. Our experimental system measures at a sampling rate of 20 GSamples/s (0.0075 m) and resolves fine structures with high accuracy. For interpretation of this received waveform a general understanding of the underlying physical principles is necessary.

In this paper, we describe investigations of the accuracy of different waveform analysis algorithms for pulse properties extraction. The experimental system for a fast recording of signals is described in section 2. In section 3, different techniques for extracting the pulse properties are discussed. The performed experiments are explained in section 4, and the obtained accuracy measurements are depicted. We conclude with a discussion about the received surface features.

2. Recording the scene

An experimental setup for exploring the capabilities to recognise urban objects using a laser system was built. For the main investigations of the influence of different object properties on the waveform, a pulsed laser system with multi photon detection was used. The measurements were carried out by an experimental setup consisting of a laser system and a captured scene with typical urban objects and materials (Figure 1).

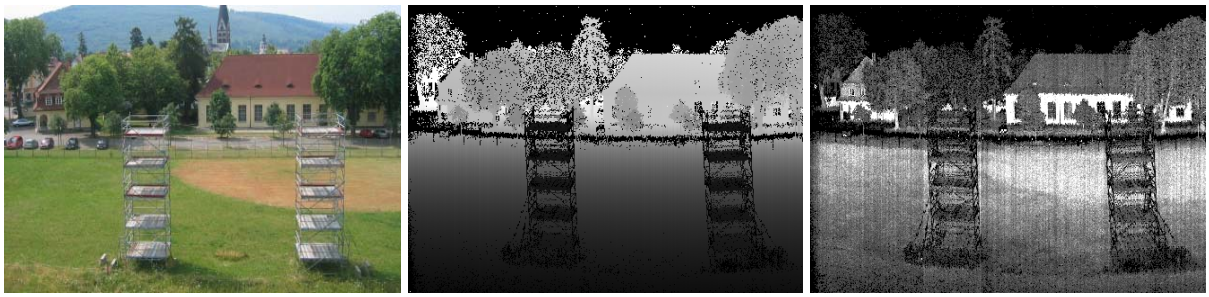

a b c

Figure 1: Images of the test scene with different urban objects.
a) digital photo, b) laser range image, c) laser reflectance image

2.1. Laser system

The laser system has three main components: an *emitter unit*, a *receiver unit*, and a *scanning unit*.

For the *emitter unit*, we use a short duration laser pulse system with a high repetition rate (42 kHz). The pulsed Erbium fibre laser operates at a wavelength of 1.55 µm. The average power of the laser is up to 10 kW and the pulse duration is 5 ns (full-width-half-maximum of the pulse). The beam divergence of the laser beam is approximately 1 mrad.

The *receiver unit* to capture the waveform is based on an optical-to-electrical converter. This converter contains an InGaAs photodiode sensitive to wavelengths of 900 to 1700 nm. Furthermore, we use a preamplifier with a bandwidth of 1 GHz and an A/D converter with 20 GSamples/s. The A/D conversion and digital recording is accomplished using a digital memory oscilloscope.

The *scanning unit* for the equidistant 2-d scanning consists of a moving mirror for elevation scan (320 raster steps of 0.1 °) and a moving platform for azimuth scan (441 raster steps of 0.1 °). The field of view is 32 ° in vertical and 44 ° in horizontal direction.

2.2. Recording the scene to a data cuboid

The experimental system is used to capture the test data used in the development of algorithms for analysing the temporal signal. The aim is to design algorithms for the assessment of an airborne laser system.

For the investigations, a measuring platform is placed at a height of 15 m, pointing at an outdoor scene. Objects in the scene are buildings, streets, vehicles, parking spaces, trees, bushes, and grass. Some objects are partly occluded and the materials show various backscattering characteristics.

For each orientation of the beam within the scanning pattern, the emitted signal and the received signal are recorded over the time t for the time interval $t=t_{min}$ to $t=t_{max}$. The time interval selected for the recording of the signal depends on the desired recording depth of the area and the expected range of the objects of interest (in our case up to 200m). For each discrete time or range value the intensity value of the pulse is stored. The entire recording of a scene can be interpreted and visualised as a discrete data cuboid $I(x,y,t)$, where the measured intensity at each time t and each beam direction (x, y) is stored. This cuboid can be interpreted in different ways. It has to be taken into account the recording geometry for correct interpretation of the data.

3. Analysing the waveform for pulse property extraction and surface features

To obtain the surface characteristics, each waveform $s(t):=s_{xy}(t)=I(x,y,t)$ of the cuboid is analysed. The surface inside the beam footprint generates a return pulse. To detect and separate these from the noise, a signal dependent threshold is estimated. Therefore the signal background noise is estimated. If the intensity of the waveform is above three times the noise standard deviation ($3\sigma_n$) for duration of at least 5 ns (full-width-half-maximum of the pulse), a pulse is assumed to be found. A section of the waveform including the pulse is passed on to the subsequent processing steps.

Typical surface features we want to extract from a waveform are *range*, *roughness*, and *reflectance*. The waveform properties corresponding to these surface features are: *time*, *width* and *amplitude*. The estimated parameters for waveform properties are the averaged time value τ (leading to an estimate for the *range*), width w (*roughness*) at full-width-half-maximum of the pulse, and maximum amplitude a (*reflectance*).

For the measurements of the test scene we assumed to receive *reflectance* values in between 10% to 80%. There are strong variations within the *reflectance* for the same material, caused by the measurement situation. These values should be used with care.

A rough surface, i.e. a surface of a certain depth, will widen the laser pulse upon reflection. Therefore, the *width* of the pulse is a clue to the surface *roughness*. Also, the widening of the

pulse causes the reflected photons to be spread over a greater amount of time, thus reducing the peak amplitude. Therefore, to estimate the *roughness* or *reflectance* features of a surface the pulse *width* and *amplitude* have to be known. Estimating just the *amplitude* of a pulse without considering this dependency will lead to inaccurate and noisy *reflectance* values.

When it comes to estimating the *roughness*, a slanted plane or a multitude of small surfaces in close proximity at slightly differing elevations (i.e. vegetation) can lead to the same observation as a rough surface. A slanted plane can be identified by examining the neighbourhood. Many small surfaces are just another description of one single rough surface, and therefore not a problem.

The pulse shape varies between measurements. Therefore, extracting the relevant properties of the waveform can be difficult. Several algorithms have been investigated, not all of them able to measure all three of the above properties. By capturing the emitted and the received waveforms for each single shot, the waveform shapes can be analysed separately and compared to each other. This has the advantage of removing the pulse shape dependence from the resulting features.

The waveform analysis offers the possibility to detect multiple pulse reflections caused by several overlapping and partly illuminated objects. This capability is not central to the studies conducted in this paper.

3.1.1. Peak algorithm

The *range* and the *reflectance* values are determined by the maximum pulse amplitude, where the highest reflectance is expected (Figure 2a). The magnitude of the maximum pulse amplitude is normalised by the maximum pulse amplitude of the emitted pulse to reduce the influence of intensity fluctuations of the laser system on the measurement. Local spikes on the pulse waveform strongly affect the feature determination. For noisy signals, a low pass filter is recommended to determine the global maxima. To measure the surface *roughness*, the width of the pulse is calculated by the full-width-half-maximum value of the pulse.

3.1.2. Leading edge algorithm

Whenever the waveform intensity rises above a predetermined threshold, a pulse is detected. The *range* is determined by the time the threshold is overshot (Figure 2b). The threshold value can be a predefined fixed value, but then the ranging detection strongly depends on the pulse waveform, amplitude, and width. We use half the maximum amplitude of the pulse as the threshold with linear interpolation of the last sub-threshold and the first super-threshold time for range determination. This ranging method gives the shortest range values.

3.1.3. Constant fraction algorithm

For *range* estimation, the pulse waveform *s(t)* is inverted, delayed for a fixed time *T*, and added to the original pulse (Figure 2c). The combined signal *c(t)* has a zero crossing point insensitive to the pulse magnitude, but depending on the pulse waveform and width [8]. We use 2.5 ns as the delay time *T*.

$$t_{CF} \Leftrightarrow c(t) = s(t) - s(t+T) = \begin{cases} t_{CF} & if \quad c(t) = 0 \\ 0 & if \quad c(t) \neq 0 \end{cases} \tag{1}$$

For symmetric pulse waveforms, the traditional constant fraction algorithm delivers good results. But, for an asymmetric noisy waveform the delayed signal should be reversed in time as well, to avoid ambiguities of the zero crossing point.

3.1.4. Centre of gravity algorithm

In this algorithm, the time value (*range*) is determined (Figure 2d) by integrating the pulse waveform *s(t)*

$$t_{CoG} = \frac{\int_0^T t\, s(t)dt}{\int_0^T s(t)dt} . \tag{2}$$

This approach delivers good results for small noise amplitudes and variable pulse waveforms.

The following methods to further process the pulse properties are not part of the Centre of gravity algorithm, but are well suited to complement it. Generally, integration over a section of the signal has the advantage of reducing the noise dependence compared to the aforementioned methods relying on single samples [9]. We call the integral of the waveform *s(t)* shown in the denominator of Equation 2 the *pulse strength*. From this, the *reflectance* value a_0 can be calculated assuming a Gaussian and using the Inverse error function (erf^{-1}) and the width *w*

$$a_0 = \frac{2\, erf^{-1}(0.5)}{\sqrt{\pi}\; w} \int_0^T s(t)dt . \tag{3}$$

Furthermore the *roughness* w_0 is approximated by the width of the central pulse area contributing 0.76 of this *pulse strength* with

$$\int_{t_{CoG}-\frac{w_0}{2}}^{t_{CoG}+\frac{w_0}{2}} s(t)dt = erf(\sqrt{\ln 2}) \int_0^T s(t)dt . \tag{4}$$

This conforms to the pulse width at full-width-half-maximum used in Section 3.1.1 and 3.1.5.

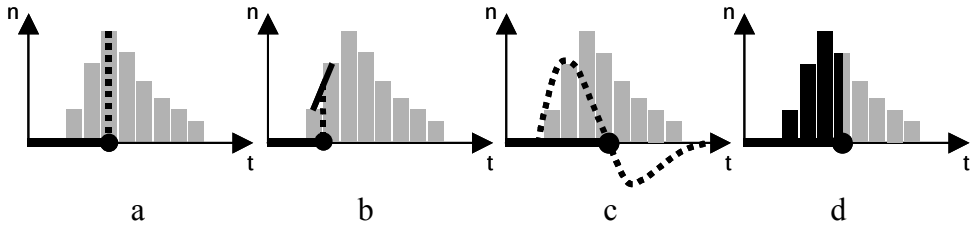

Figure 2: Algorithms for feature extraction. a) peak detection, b) leading edge detection, c) constant fraction detection, d) centre of gravity detection

3.1.5. Levenberg-Marquardt algorithm

Here, the recorded waveform *s(t)* of the pulse is approximated by a Gaussian *g(t)* to get a parametric description. Fitting a Gaussian to the complete waveform has the advantage of decreasing the influence of noise and waveform fluctuation. To estimate the relevant waveform properties of the structures the Levenberg-Marquardt optimization algorithm [10] with iterative parameter estimation is used. The estimated parameters for waveform properties are the averaged time value τ, width *w* at full-width-half-maximum of the pulse, and maximum amplitude *a*:

$$g(t) = a \exp(-\frac{(t-\tau)^2}{w^2} 4 \ln 2) \tag{5}$$

This method requires an initial value (τ_0, w_0, a_0) of the parameter vector to be estimated. We use the time of the pulse maximum for τ_0, the width of the signal at half pulse height[1] for w_0 and the value of the of the pulse maximum for a_0.

3.1.6. Correlation algorithm

The correlation algorithm, also known as *matched filter* has been developed with radar signals in mind [11] and is now a well-known part of general systems theory [12,13].

The correlation is computed by the cross-correlation R_{XS} between the waveform of the emitted pulse x and the received waveform s. We obtain the output waveform y with a local maximum at the delay time τ.

$$y(t) = R_{xs}(t-\tau) \tag{6}$$

Then the output waveform with improved *SNR* is analysed by a detection filter for local maxima to determine the travel time of the pulse. By using the correlation signal for processing the travel time a higher accuracy is reached than by operating on the waveform. This is because the specific pulse properties (e.g. asymmetric shape, spikes) are taken into account and so less temporal jitter can be expected. For the detection the preservation of the waveform has no relevance, only maximizing the *SNR* is important.

Furthermore, the range resolution of the laser system generally depends on the temporal width of the emitted pulse waveform. Short pulse waveforms decrease the average signal power and the associated *SNR*. To increase the temporal waveform width without decreasing range resolution we need to consider waveform compression. The typical time-bandwidth product of a conventional system is $BT \approx 1$, but with an increasing bandwidth B of the receiver and a corresponding waveform the range resolution ΔR is increased and we obtain with the speed of light c

$$\Delta R = \frac{c}{2B} \tag{7}$$

Then the improved range resolution of the laser system is inversely proportional to the bandwidth.

4. Experiments

The experiments are carried out to investigate the reliability and quality of feature extraction. The data is recorded with a laser system by measuring the same scene at different time stamps and proof the accuracy by the received multiple measurements. The measured surface features are compared with each other. The scene includes a mixture of man made objects and vegetation. For our investigations the relative accuracy between the measurements is proofed.

Two data cuboids of the same scene with a short time shift were recorded. The data cuboids were analysed by the algorithms mentioned above and for each detected pulse the surface

[1] The Gaussian has a width of $w_0 = \sigma\sqrt{8\ln 2}$ at one half of its maximum height. Therefore, the σ of any given Gaussian is approximately 0.42 times this width. We choose this particular height to get a feature that is as robust as possible.

features *range*, *roughness*, and *reflectance* are determined. To compare the accuracy of determining surface features the corresponding pulses of the same illuminated surface for both measurements have to be found. The corresponding pair has to be below a given threshold in distance (0.5 m) to avoid outliers. Then the determined pair of pulses from the two measurements should depend on the same illuminated area with the same surface characteristic. Ideally they should deliver the same surface features.

Depending on the area size in relation to the beam footprint it is possible, that the complete pulse intensity is backscattered from the first illuminated surface in propagation direction. The following surfaces give only poor or none reflections. For instance, a tree with dense foliage caused by the summer season may return only a single reflection response per laser pulse illumination.

4.1.1. Accuracy of measuring the range

Because of the strong fluctuation in the temporal shape from pulse to pulse the emitted and the received waveforms are processed by the algorithms as described in Section 3. The difference of the relative range value between the emitted and each received waveform per single shot is used to determine the absolute *range* value. The difference in *range* between both measurements for relative accuracy is determined and accumulated in a histogram. Figure 3 shows the histograms for the derived range differences of the investigated algorithms.

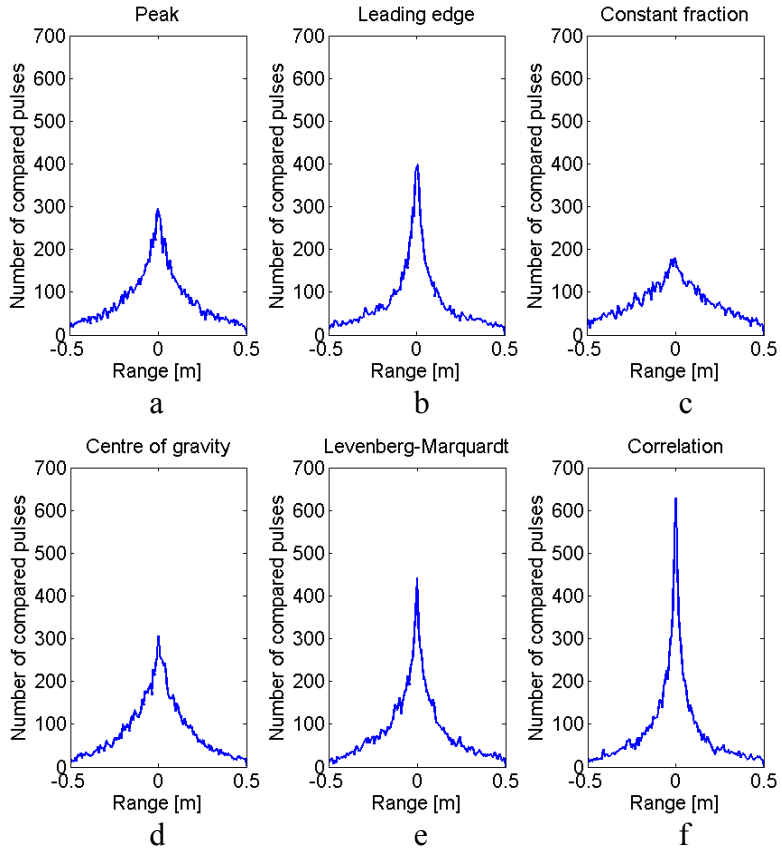

Figure 3: Difference histograms for the feature *range* of the investigated algorithms

Furthermore the standard deviation of difference in *range* for each algorithm is processed (Table 1). The analysis shows that the correlation (Figure 3f) reaches the best result, followed by the Levenberg-Marquardt algorithm (Figure 3e). The leading edge algorithm provides

good results caused by the steepness of the pulse waveform from the used laser system (Figure 3b). Poor accuracy performs the constant fraction algorithm (Figure 3c). The constant fraction could probably give better results if the noisy waveform would be low pass filtered. The average value of difference in *range* for all investigated algorithms is below 1 cm.

4.1.2. Accuracy of measuring the roughness

To determine the *roughness* by the width of the pulse the received waveforms are investigated and the difference between the measurements is determined. Physically the width for the received pulses stays the same for a plane surface illuminated perpendicular to the beam propagation or increases for rough or slant surfaces. In Figure 4 the results of the roughness differences of the investigated algorithms are depicted.

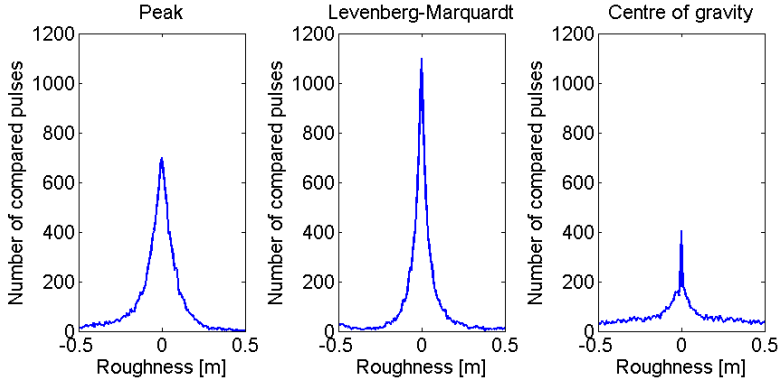

Figure 4: Difference histograms for the feature *roughness*

In Table 1 is shown that the Levenberg-Marquardt algorithm (Figure 4b) delivers the best standard deviation of difference in *roughness* followed by the peak algorithm (Figure 4a) and the centre of gravity (Figure 4c). Even with the used high sampling rate it can be said that this feature is most difficult to estimate because of the small variations in between the single pulse measurements.

Algorithm \ Standard deviation	*Range* [m]	*Roughness* [m]	*Reflectance* [%]
Peak	0.200	0.128	5.453
Leading edge	0.190	-	-
Constant fraction	0.223	-	-
Centre of gravity	0.190	0.231	8.184
Levenberg-Marquardt	0.185	0.121	4.902
Correlation	0.173	-	-

Table 1: Relative feature accuracy comparing two measurements of the same scene

4.1.3. Accuracy of measuring the reflectance

To determine the *reflectance* by the amplitude of the pulse the received waveforms are investigated. The amplitude values are converted to *reflectance* values by assuming values in between 10% to 80%. The difference between the measurements is calculated and the relative accuracy is accumulated in a histogram. Figure 5 shows the histograms for the derived reflectance differences of the investigated algorithms.

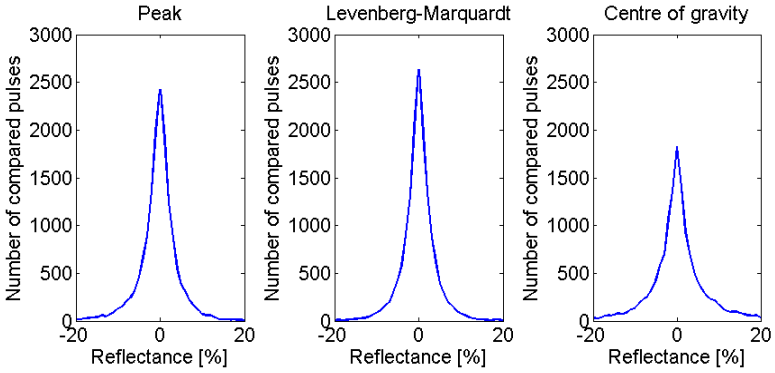

Figure 5: Difference histograms for the feature *reflectance*

The standard deviation of difference in *reflectance* for each algorithm is processed (Table 1). In Table 1 is shown that the Levenberg-Marquardt (Figure 5b) delivers a slightly better result then the peak algorithm (Figure 5a) followed by the centre of gravity (Figure 5c).

5. Discussion

In this investigation we illuminate each surface twice. This gives the possibility to assess the measurement itself. Errors by inaccuracy of the used scanner unit can appear and decreases the accuracy of the achieved results. The minimum value which could be distinguished in step of range for all investigated algorithms on the scene was better than 1 cm. The highest accuracy for *range* extraction could be reached by the correlation method using the waveform of the emitted and the received pulse (Table 1). This shows that analysing the emitted and the received signal has the advantage of removing the pulse shape dependence for gaining range accuracy. In general the methods using the shape of the signal (Levenberg-Marquardt, correlation) to extract the range value give the best results (compare with Table 1 and Figure 3e,f) followed by the method using more than a single value (centre of gravity). The poorest results were reached by using a single value (peak, leading edge, constant fraction).

Analysing the surface feature *roughness* and *reflectance* the accuracy could be gained by the Levenberg-Marquardt algorithm (Table 1), because it considers the shape of the signal. Surprising and difficult to explain in these cases is the poor accuracy of the centre of gravity compared to the peak algorithm (Figure 4a,c and 5a,c). Integration over the signal should give better results than processing only single values of the signal. The feature roughness includes different elevated object surfaces within the beam corridor which lead to a mixture of different range values and increase the pulse width. This may be caused by a slanted plane, or vegetation like branches and leaves of a tree. However the amount of reflected photons is given by the pulse width and amplitude. An increasing pulse width leads to a decreasing pulse amplitude value and vice versa for the same number of photons. Therefore, for estimating the roughness or reflectance features of a surface the pulse width and amplitude have to be known. Only estimating amplitude of a pulse without considering this dependent will lead to inaccurate and noisy reflectance values.

The results we achieved by the experiments are valid for our system, but for general investigations they can be used to optimise pulsed laser systems. We investigated a scene with typical urban objects and materials. For other type of objects (e.g. glacier or specific plants) the analysis can be adapted.

6. Conclusion

We have shown that exploiting the shape of the pulse waveform instead of a single value for extracting surface features increases the accuracy. In our case for feature extraction the best results are gained by a combination of correlation and Levenberg-Marquardt method. Depending on the waveform of the used laser system the waveform analysis provides the possibility to use specific pulse properties extraction to gain the relevant surface properties by special algorithms. In future research it has to be examined whether the gained surface features offers robust analysis methods for specific applications or not.

7. Acknowledge

We thank Hanno Lutterman and Olaf Mäder for assistance during the measurement campaign.

References:

[1] Huising E.J., Gomes Pereira L.M.: Errors and accuracy estimates of laser data acquired by various laser scanning systems for topographic applications. ISPRS Journal of Photogrammetry & Remote Sensing 53: 245-261, 1998.

[2] Wehr A., Lohr U.: Airborne laser scanning – an introduction and overview. ISPRS Journal of Photogrammetry & Remote Sensing 54: 68-82, 1999.

[3] Baltsavias E.P.: Airborne laser scanning: existing systems and firms and other resources. ISPRS Journal of Photogrammetry & Remote Sensing 54: 164-198, 1999.

[4] Jutzi B., Stilla U.: Laser pulse analysis for reconstruction and classification of urban objects. In: Ebner H., Heipke C., Mayer H., Pakzad K. (eds) Photogrammetric Image Analysis PIA'03. International Archives of Photogrammetry and Remote Sensing. Vol. 34, Part 3/W8, 151-156, 2003.

[5] Jutzi B., Eberle B., Stilla U.: Estimation and measurement of backscattered signals from pulsed laser radar. In: Serpico S.B. (ed) (2003) Image and Signal Processing for Remote Sensing VIII, SPIE Proc. Vol. 4885: 256-267, 2002.

[6] Wagner W., Ullrich A., Melzer T., Briese C., Kraus K.: From single-pulse to full-waveform airborne laser scanners: Potential and practical challenges. In: Altan M.O. (ed) International Archives of Photogrammetry and Remote Sensing. Vol 35, Part B3, 201-206, 2004.

[7] Jutzi B., Stilla U.: Extraction of features from objects in urban areas using space-time analysis of recorded laser pulses. In: Altan M.O. (ed) International Archives of Photogrammetry and Remote Sensing. Vol. 35, Part B2, 1-6, 2004.

[8] Kamermann G.W.: Laser Radar. In: Fox C.S. (ed) Active Electro-Optical Systems, The Infrared & Electro-Optical Systems Handbook. Michigan: SPIE Optical Engineering Press, 1993.

[9] Vosselman G.: On estimation of planimetric offsets in laser altimetry data. Vol. XXXIV, International Archives of Photogrammetry and Remote Sensing: 375-380, 2002.

[10] Hartley R., Zisserman A.: Multiple View Geometry in Computer Vision. Proc. Cambridge University Press, Cambridge, 2000.

[11] Skolnik M.I.: Introduction to radar systems. McGraw-Hill International Editions, Second Edition, 1980.

[12] Papoulis A.: Probability, Random Variables, and Stochastic Processes. Tokyo: McGraw-Hill, 1984.

[13] Unbehauen R.: Systemtheorie 1. Oldenbourg Verlag, München, 7. Auflage, 1996.